

Nonlinear propagation of ultrasound through varying contrast-agent concentrations

B. Hermens¹, M. Mischi¹, M. Böhmer², R.M. Aarts^{1,2}, H.H.M. Korsten^{1,3}

¹Eindhoven University of Technology, Department of Electrical Engineering, the Netherlands

²Philips Research, Eindhoven, the Netherlands

³Catharina Hospital, Eindhoven, the Netherlands

Abstract: Several methods are becoming available that permit the extraction of quantitative data by means of contrast echography. To this end, an accurate quantification of the concentration of diluted contrast agent is required. In order to improve the method sensitivity, dedicated imaging modes, which detect the nonlinear behavior of contrast agents, are often used. However, the imaging effects of the nonlinear propagation of ultrasound (US) through contrast dilutions are never taken into account. In this paper, the nonlinear distortion of US is analyzed for varying concentrations of the Luminy® contrast agent. The analysis focuses on the influence of the nonlinear distortion on the contrast-to-tissue ratio (CTR), which is typically used to determine the performance of contrast enhancement imaging modes. A dedicated set-up was built for the measurements. The presented nonlinear analysis is based on the Burger's equation. The results show an increase of US distortion for increasing contrast concentration. Despite the simplicity of the adopted model, the resulting fits were accurate, proving that the model is suitable to describe the distortion of US for varying Luminy® concentrations.

Introduction

Several echographic applications are based on the intravenous injection or infusion of an ultrasound contrast agent (UCA) and its subsequent detection in the region to be investigated. Dedicated applications have been developed to analyze the perfusion of organs as well as for the assessment of global cardiovascular parameters [1-3].

UCAs are microbubbles of gas enclosed in a biocompatible shell [4]. In order to improve the contrast detection, several contrast enhancement imaging modes have been developed in the last decade [5]. These methods exploit the nonlinear backscatter of UCA, which differs from the approximately linear backscatter of tissue.

Together with the backscatter, the propagation of ultrasound (US) through UCA dilutions is also nonlinear, resulting in a number of implications that are often ignored. An important example is given by

the contrast-to-tissue ratio (CTR), which is considered as a measure for the performance of contrast enhancement imaging modes [6]. The determination of the CTR is usually based on independent measurements of backscatter from UCA dilutions and tissue, while the interaction between the two systems is not considered [6].

In this paper, an analysis of the nonlinear propagation and distortion of US through UCA is presented. Differently from previous work [7], showing the effects of nonlinear propagation at different frequencies and pressures, we focus on the nonlinear propagation effects for varying UCA concentrations. These effects may be relevant for the accurate application of perfusion and dilution quantification methods.

The adopted UCA is Luminy® (Bristol Myers Squibb). A dedicated set-up is built to analyze the effects of nonlinear propagation on the spectrum of the US waves as well as on specific contrast enhancement pulse schemes, such as power modulation (PM).

The US propagation nonlinearity is modeled by the solutions of the Burger's equation, adapted to the different conditions (e.g., UCA concentrations) [8, 9].

Methodology

Experimental set-up

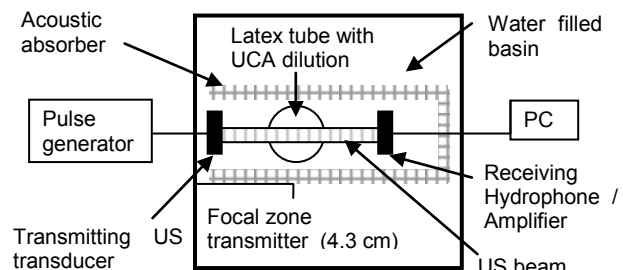


Figure 1, Experimental set-up.

The set-up in Fig. 1 was realized and used for the measurement of the nonlinear distortion of US waves propagating through UCA. The set-up consisted of a single element transducer (Olympus) aligned with a

hydrophone (Onda), both submerged in a water filled tank. The US transducer was driven by a pulse generator (Agilent) and an RF amplifier (ENI). Latex tubes containing different UCA dilutions were placed in the focal zone of the transducer for maximum efficiency.

The signal from the hydrophone was sampled by a 100 MHz A/D converter (National Instruments). The maximum sample frequency was used to ensure that the Nyquist limit was fulfilled up to the fourth harmonic.

All measurements were performed using a low MI of 0.1 and Luminity® concentrations between 0 $\mu\text{L/L}$ and 18 $\mu\text{L/L}$. This is the range where a linear relationship was observed between acoustic backscatter and Luminity® dilutions [10]. This concentration range is therefore suitable for perfusion and dilution quantitative studies. Two frequencies, 1 and 1.5 MHz, were used. These frequencies are close to the resonance frequency of the adopted transducer and Luminity® (1.5 MHz) [11].

Two different US sequences were used for the measurements. A ten period sinusoidal wave, which was used for the frequency analysis of the distorted US and a specific sequence of three pulses, which implemented a typical power modulation scheme for contrast detection. The first and last pulse had a peak pressure that was half of that of the second pulse. Each pulse was a single sinusoidal cycle and the delay between the pulses was 13 μs (Fig. 2). In order to detect the contrast nonlinearity, the reflections of a side pulse are multiplied by two and subtracted from the reflections of the central pulse.

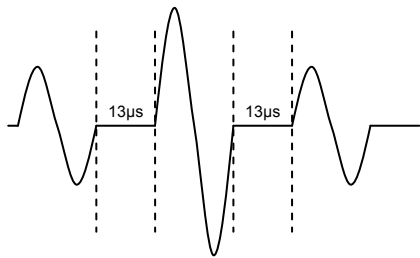


Figure 2. US sequence of three pulses that reproduced a power modulation scheme.

Signal analysis

Prior to the analysis, the measured signals were low pass filtered to suppress unwanted energy above the fourth harmonic. After this, the segment containing the US pulses was extracted using a Hamming window to minimize frequency leakage.

For the frequency analysis of the 10 pulse bursts, the extracted US signal was transformed to the frequency domain using a fast Fourier transform.

The energy at each harmonic was calculated by integrating the power spectrum in a small bandwidth about the central frequency. This bandwidth was determined at the 3dB drop of the spectrum energy. All the analysis was implemented in MATLAB (The Mathworks).

Next to the frequency analysis, a time domain analysis of the nonlinear distortion was also performed using a physical model to estimate the attenuation (α) and nonlinearity coefficient (β) characterizing the US propagation through the Luminity® dilutions.

The adopted physical model is based on the Burger's differential equation [8]. It is given as

$$\frac{\partial P}{\partial x} + \delta \cdot \frac{1}{2} \cdot c_0^{-3} \cdot \frac{\partial^2 P}{\partial \tau^2} = -\beta \cdot P \cdot (\rho_0 \cdot c_0^3)^{-1} \frac{\partial P}{\partial \tau}, \quad (1)$$

where P represents the acoustic pressure variations (Pa), x the distance (m), δ the US diffusivity (m^2s^{-1}), c_0 the equilibrium US velocity (ms^{-1}), ρ_0 the equilibrium density (kg m^{-3}), and τ a time parameter referred to as slow time parameter [8].

The Burger's equation and the nonlinear propagation model are derived under the assumption that all terms of order three or higher are small compared to the second order and, therefore, negligible [8].

An exact solution of the Burger's equation is derived when either the attenuation or the nonlinearity is zero [8]. Otherwise, the solution has to be approximated. An approximated solution can be written as

$$P(x, \tau) = P_0 \cdot \sum_{n=1}^{\infty} B_n(x) \sin(n \cdot \omega \cdot \tau), \quad (2)$$

where ω represents the angular frequency. The different spectral amplitudes (B_n) can be approximated depending on the ratio between attenuation and nonlinearity, which is determined using the Gol'dberg number Γ [8].

In case $\Gamma < 1$ (attenuation more dominant than nonlinearity), the spectral amplitudes B_n can be expressed as [9]

$$\begin{cases} B_1 = e^{-\alpha \cdot x} - \frac{1}{32} \cdot \Gamma^2 \cdot e^{-\alpha \cdot x} \cdot (1 - e^{-2 \cdot \alpha \cdot x}) + O(\Gamma^4), \\ B_2 = \frac{1}{4} \cdot \Gamma \cdot (e^{-2 \cdot \alpha \cdot x} - e^{-4 \cdot \alpha \cdot x}) + O(\Gamma^3) \\ B_3 = \frac{1}{32} \cdot \Gamma^2 \cdot (2e^{-3 \cdot \alpha \cdot x} - 3e^{-5 \cdot \alpha \cdot x} + e^{-9 \cdot \alpha \cdot x}) + O(\Gamma^4) \end{cases} . \quad (3)$$

In case $\Gamma \gg 1$ (nonlinearity more dominant than attenuation), the spectral amplitudes B_n can be expressed as [8]

$$B_n = \frac{2 \cdot \Gamma^{-1}}{\sinh(n \cdot (1 + \sigma) \cdot \Gamma^{-1})}, \quad (4)$$

where σ is the normalized distance parameter [8]. The solutions in (3) and (4) permit to derive the attenuation coefficient α and the coefficient of nonlinearity β [8]. We may assume that the estimated values for α and β represent the attenuation and nonlinearity due to UCA, because of the low attenuation and nonlinearity of water [8].

For increasing concentrations of Luminity®, the attenuation is expected to increase. For concentrations above $13.5 \mu\text{L/L}$, the measured signal is expected to show a fast decay due to the appearance of shadowing [10], i.e., the UCA attenuation impedes the propagation of US energy. The nonlinearity is also expected to increase for increasing Luminity® concentrations.

In addition to the analysis of the 10 cycle bursts in the frequency and time domain, also an evaluation of the power modulation scheme was performed. The signal was evaluated to quantify its increase due to propagation through UCA. An increase corresponds to imaging artifacts and a decrease of the CTR.

Results

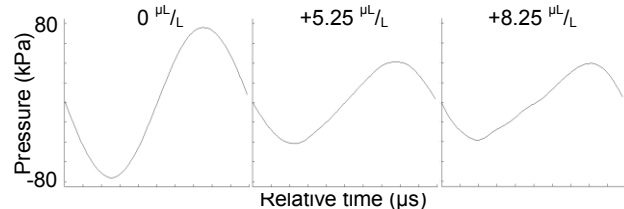


Figure 3. Nonlinear US distortion for increasing Luminity® concentration, most left $0 \mu\text{L/L}$, centre $5.25 \mu\text{L/L}$, and right $13.5 \mu\text{L/L}$. 1 MHz measurement.

As expected, the results show an increase of US distortion as the Luminity® concentration increases. The first noticeable consequence is an increase of the propagation velocity for compressive waves with respect to rarefactional waves, which results in a saw-shaped waveform, shown in Fig. 3 [8].

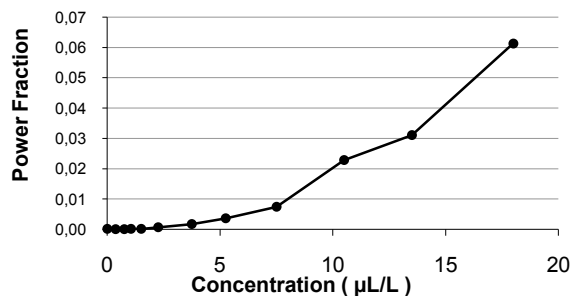


Figure 4. Normalized second harmonic power for the 1 MHz measurement.

In general, we observed a clear increase of the energy at the second harmonic (Fig. 4). The increase at other frequencies (sub-, ultra-, and super-harmonic) was much less significant. This result confirms the second order assumption made for the derivation of the nonlinear model. This assumption was also confirmed by the limited increase of the accuracy of the model fit (1% more accurate for the highest concentrations), when a third order model was tested.

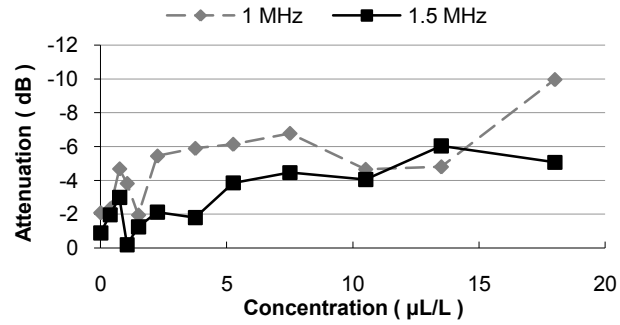


Figure 5. Attenuation for increasing Luminity® concentrations.

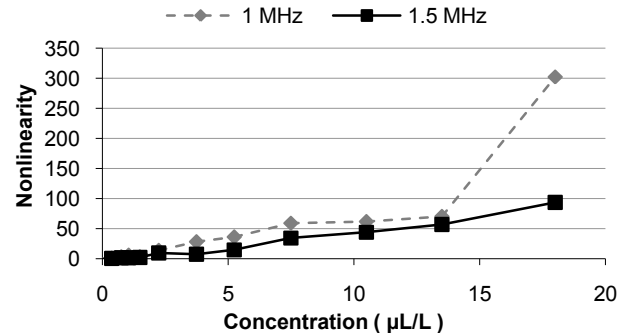


Figure 6. Nonlinearity for increasing Luminity® concentrations modeled for $\Gamma < 1$.

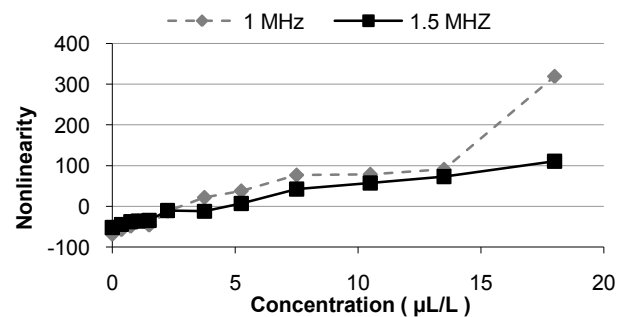


Figure 7. Nonlinearity for increasing Luminity® concentrations model for $\Gamma \gg 1$.

The fit of the model showed a mean determination coefficient $r^2 = 0.99$. At both frequencies, 1 and 1.5 MHz, an approximately linear increase of attenuation and nonlinearity for increasing Luminity® concentration was observed (Fig. 5-7).

For concentrations below $3.75 \mu\text{L/L}$, the attenuation and nonlinearity coefficients, α and β , estimated

under the assumptions $\Gamma < 1$ and $\Gamma \gg 1$ showed a large deviation. For low concentrations, in fact, $\Gamma < 1$ and the solution to the Burger's equation for $\Gamma \gg 1$ is not suitable. Beyond $3.75 \mu\text{L/L}$, the values of α and β estimated by both solutions, (3) and (4), were closer to each other. The results are shown in Fig. 6 and 7.

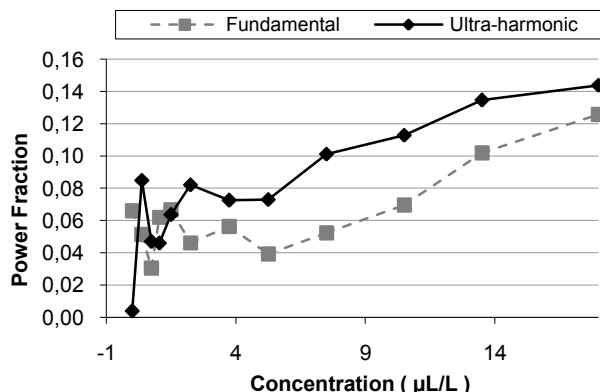


Figure 8, Power modulation energy at fundamental and ultra-harmonic frequencies for the 1 MHz pulses.

Concerning the power modulation analysis, the use of the last two pulses of the power modulation sequence showed the lowest increase of energy at the fundamental frequency for increasing Lumintensity® concentrations (Fig. 8), corresponding to the smallest nonlinear distortion. This condition would therefore limit the CTR reduction due to nonlinear distortion. The strongest increase of the signal energy was found using the first two pulses at the ultra-harmonic frequency. This is therefore the condition that results in the most significant distortion of the ultrasonic waves.

Discussion and conclusions

The increase of spectral power is most significant for the second harmonic frequency.

The small increase of the accuracy of the model fit, found using a third order version of the model, shows that the second order assumption is justified. This is also confirmed by the accurate fits of the second order model to the measurements.

The attenuation and nonlinearity coefficient for Lumintensity® concentrations up to $3.75 \mu\text{L/L}$ should be derived by using the model for $\Gamma < 1$. For concentrations higher than $3.75 \mu\text{L/L}$, the Gol'dberg number slowly increases, but stays close to 1 (max $\Gamma = 7$). Due to the small Gol'dberg number, the model for $\Gamma < 1$ can be used for the entire range of Lumintensity® concentrations that was adopted. Further research could focus on the integration of the solutions to improve the accuracy of the estimation of the attenuation and nonlinearity coefficient.

Regarding the power modulation scheme, the energy increase is most significant at ultra harmonic frequency using the first two pulses. For further measurements, two period pulses could be used to reduce the influence of the transducer transitory states.

In general, the results show that the Burger's equation can already provide an accurate description of the nonlinear propagation of US through contrast media. This conclusion needs however to be confirmed for different frequencies, where diffraction or resonance effects might be more evident and bubble dynamics might need to be incorporated in the model.

References

- [1] M. Mischi, A. H. M. Jansen, and H. H. M. Korsten, "Identification of cardiovascular dilution systems by contrast ultrasound," *Ultrasound in Med. & Biol.*, vol. 33, pp. 439-451, 2007.
- [2] K. Wei, A. R. Jayaweera, S. Firoozan, A. Linka, D. M. Skyba, and S. Kaul, "Quantification of myocardial blood flow with ultrasound-induced destruction of microbubbles administrated as a constant venous infusion," in *Circulation*, vol. 97, 1998, pp. 473-483.
- [3] M. Krix, C. Plathow, F. Kiessling, F. Herth, A. Karcher, M. Essig, H. Schmitteckert, H. U. Kauczor, and S. Delorme, "Quantification of perfusion of liver tissue and metastases using a multivessel model for replenishment kinetics of ultrasound contrast agents," *Ultrasound in Med. & Biol.*, vol. 30, pp. 1355-1363, 2004.
- [4] H. Becher and P. N. Burns, *Handbook of contrast echocardiography*. Frankfurt and New York: Springer Verlag, 2000.
- [5] P. J. A. Frinking, A. Bouakaz, J. Kirkhorn, F. J. T. Cate, and N. de Jong, "Ultrasound contrast imaging, current and new potential methods," in *Ultrasound in Med. and Biol.*, vol. 26, 2000, pp. 965-975.
- [6] A. Bouakaz, S. Frigstad, N. de Jong, and F. J. Ten Cate, "Super harmonic imaging: a new imaging technique for improved contrast detection," *Ultrasound in Med. and Biol.*, vol. 28, pp. 59-68, 2002.
- [7] M. Tang and R. Eckersley, "Nonlinear propagation of ultrasound through microbubble contrast agents and implications for imaging," *IEEE Trans Ultrasonics Ferroelectrics Frequency Control*, vol. 53, pp. 2406-15, 2006.
- [8] M. Hamilton and D. Blackstock, *Nonlinear Acoustics*. San Diego: Academic Press, 1997.
- [9] D. Blackstock, "Connection between the Fay and Fubini solutions for plane waves of finite amplitude in a viscous fluid," *The journal of the acoustic society of America*, vol. 39, pp. 1019-1026, 1966.
- [10] S. Yamada, K. Komuro, M. Taniguchi, and A. Uranishi, "A fundamental study for quantitative measurement of ultrasound contrast concentration by low mechanical index contrast ultrasound," *J. Med. Ultrasonics*, vol. 33, pp. 77-83, 2006.
- [11] V. Sboros, C. Moran, S. Pye, and W. McDicken, "An in vitro study of a microbubble contrast agent using a clinical ultrasound imaging system," *Physics in Medicine and Biology*, vol. 49, 2004.